SUPPLEMENTARY FIGURES

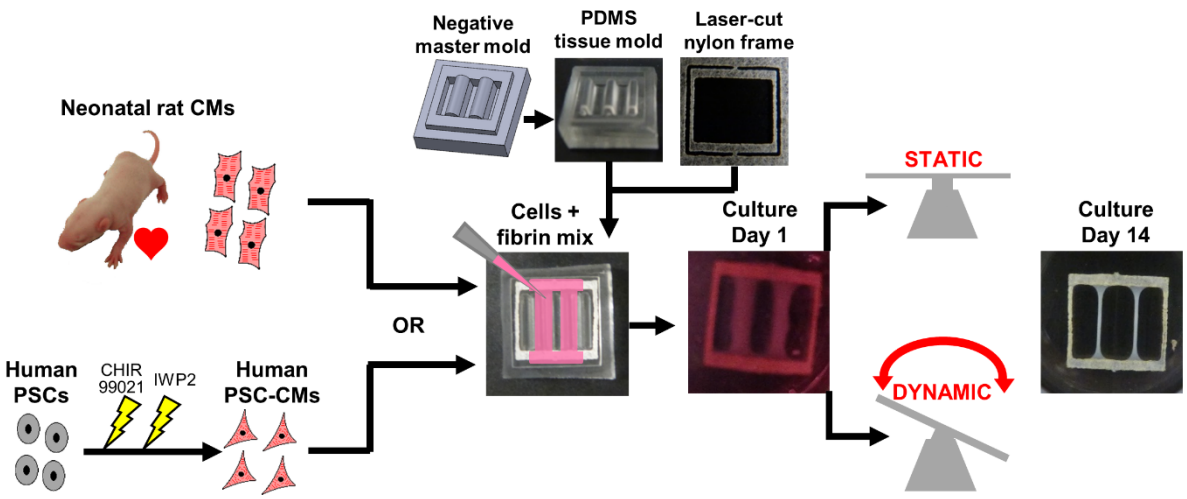

Figure S1: Schematic of cardiobundle fabrication and culture.
Neonatal rat CMs or differentiated human PSC-CMs were embedded in a fibrin-based hydrogel and cast into a PDMS tissue mold with cylindrical troughs to form bundle-shaped tissues. Ends of the 7mm-long cardiobundles were attached to a surrounding frame composed of porous nylon mesh, with 2 cardiobundles cultured per frame. One day after cardiobundle fabrication, the frame and cardiobundles were removed from the PDMS tissue mold and cultured on a static or dynamic (rocking) platform.

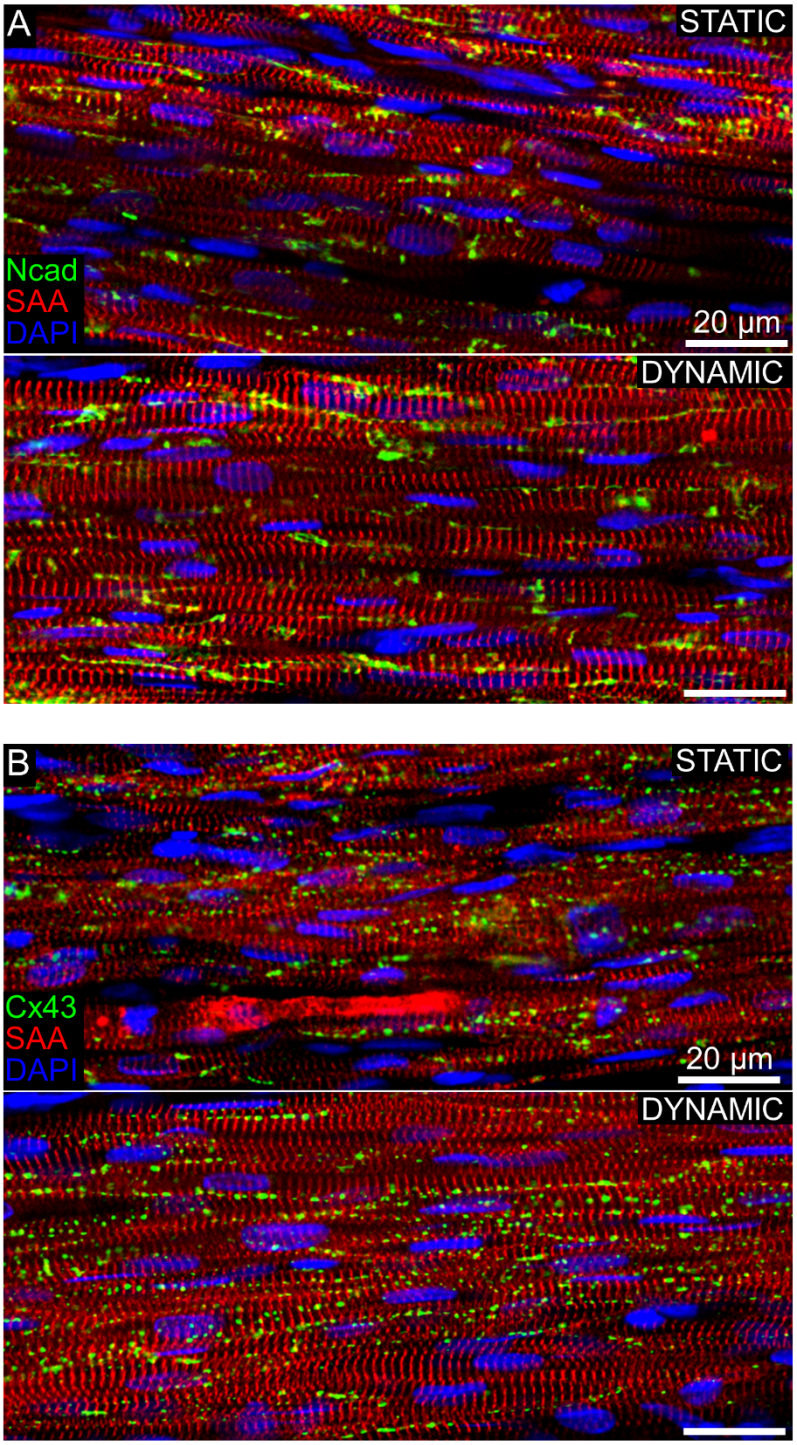

Figure S2: Electrical and mechanical junctions in NRVM cardiobundles.
(A) Representative longitudinal sections of NRVM cardiobundles cultured for 2 weeks under static or dynamic conditions, stained for N-cadherin (Ncad, green), Sarcomeric α-actinin (SAA, red), and nuclei (DAPI, blue). **(B)** Representative 2-week cardiobundles stained for Connexin 43 (Cx43, green), SAA (red), and nuclei (blue).

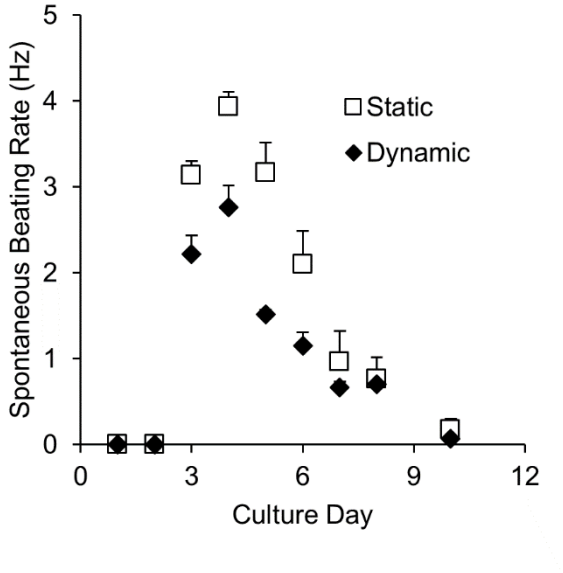

Figure S3: Spontaneous beating rate of statically and dynamically cultured NRVM cardiobundles as a function of culture time.
n = 6 cardiobundles per group from 2 cell isolations.

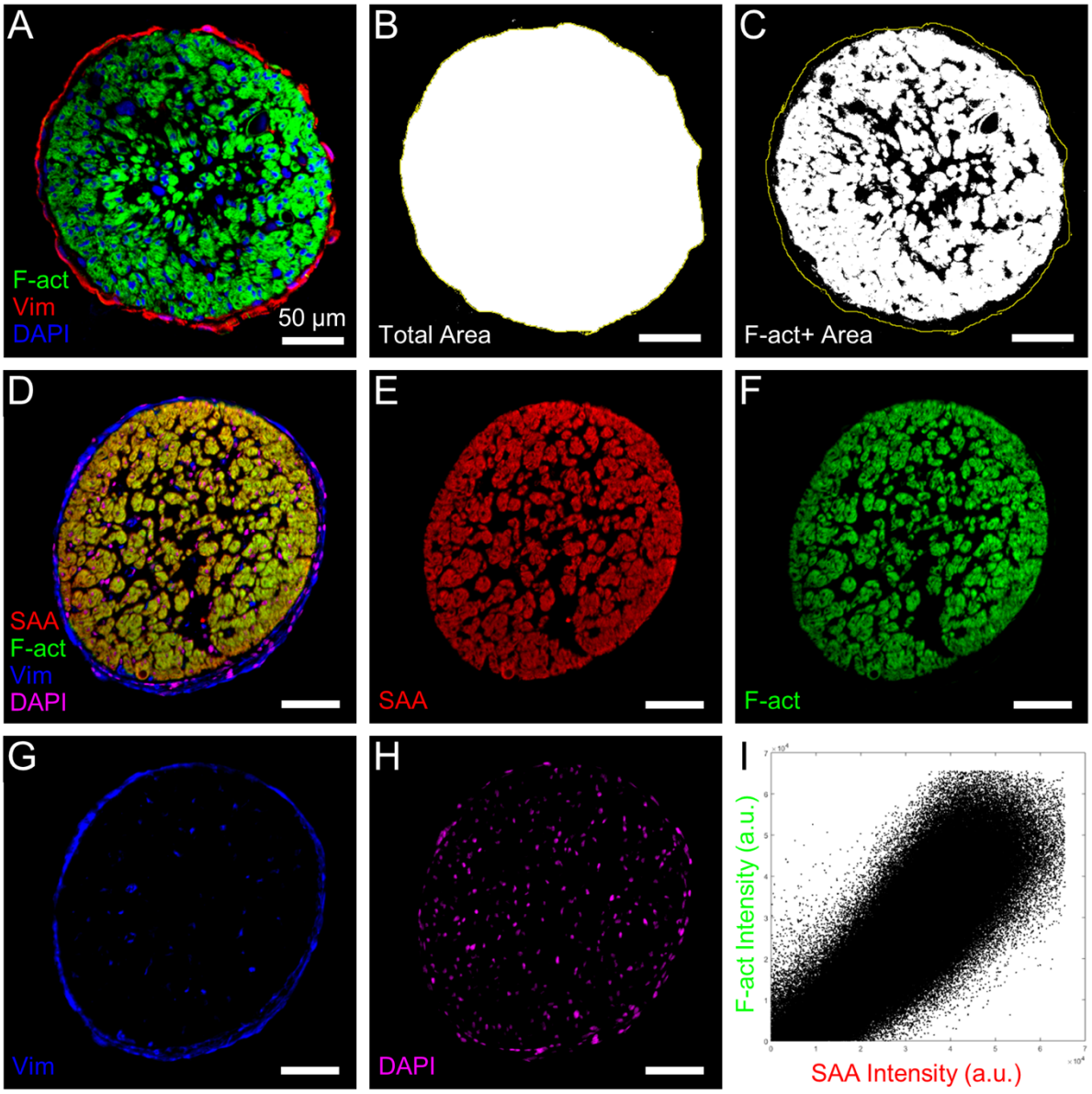

Figure S4: Image analysis of cardiobundle transverse cross-sections.
(A) Representative transverse cross-section of NRVM cardiobundle cultured dynamically for 2 weeks, stained for F-actin (F-act), vimentin (Vim), and nuclei (DAPI). **(B)** Total cross-sectional area represents a highlighted region with the outer boundary of the merged image in (A); see "Immunostaining and Image Analysis" section of Supplementary Methods. **(C)** Highlighted F-act^{+} area was measured by thresholding green channel of the image in (A). Yellow line demonstrates the outer boundary identified in (B). **(D)** Representative transverse cross-section of another NRVM cardiobundle cultured dynamically for 2 weeks, stained for myocyte-specific sarcomeric α-actinin (SAA), F-act, Vim, and DAPI. **(E-H)** Individual color channels of image shown in (D). **(I)** Scatterplot of F-act intensity (green channel) vs. SAA intensity (red channel) for pixels of the image in (D). Average Pearson correlation coefficient from analysis of n = 4 cardiobundles had value of 0.920 ± 0.031, demonstrating near-perfect overlap of F-actin and SAA staining.

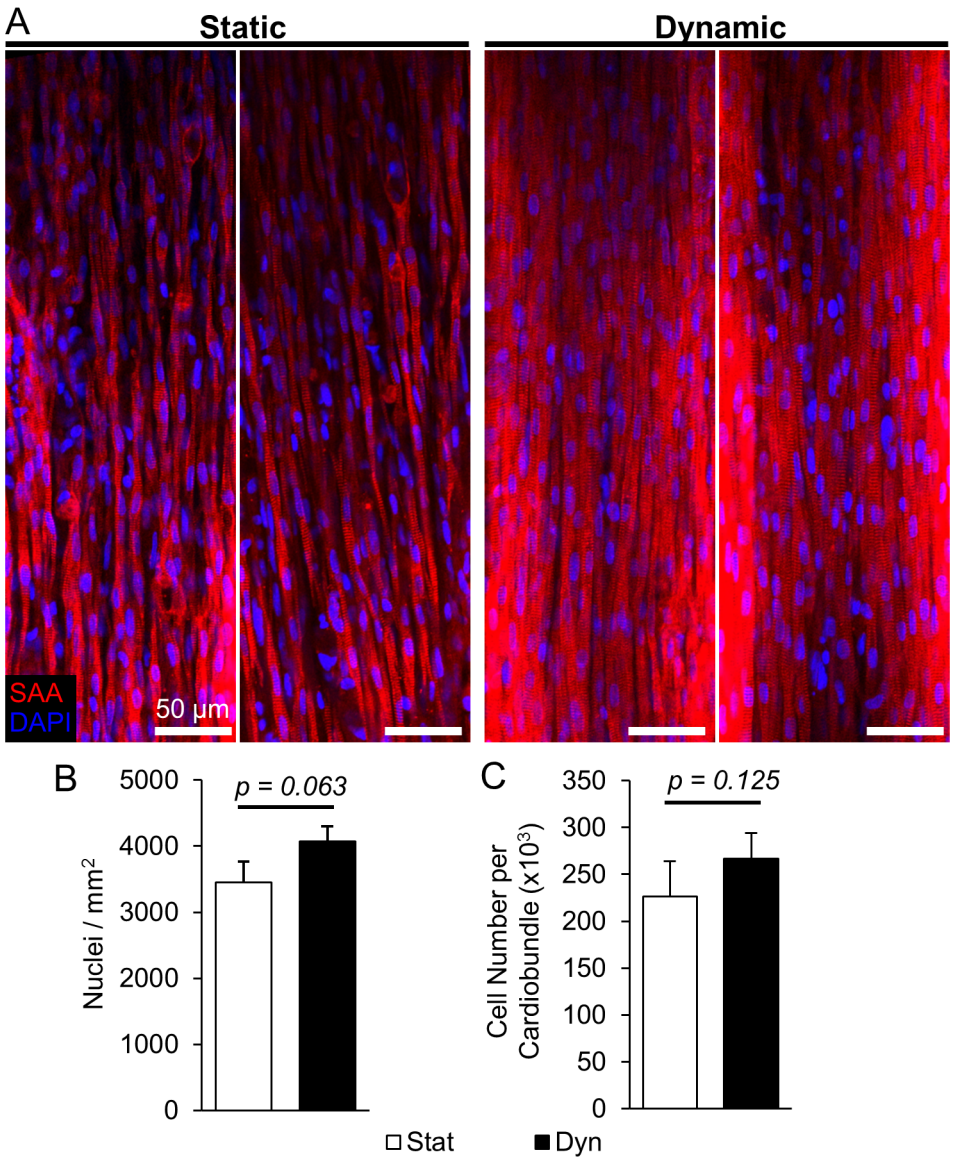

Figure S5: Additional assays for evaluation of nuclear count in NRVM cardiobundles.
(A) Two representative longitudinal sections, each of statically and dynamically cultured 2-week NRVM cardiobundles stained for sarcomeric α-actinin (SAA) and nuclei (DAPI). **(B)** Nuclei per mm^2 counted from longitudinal images (n =10 – 14 cardiobundles per group from 2 cell isolations). **(C)** Cell number per cardiobundle measured by Hoechst assay for quantifying total DNA (n = 12 cardiobundles per group from 2 cell isolations). Cell suspension used for making cardiobundles was lysed and serially diluted to create a standard curve of DNA amount vs. known cell number.

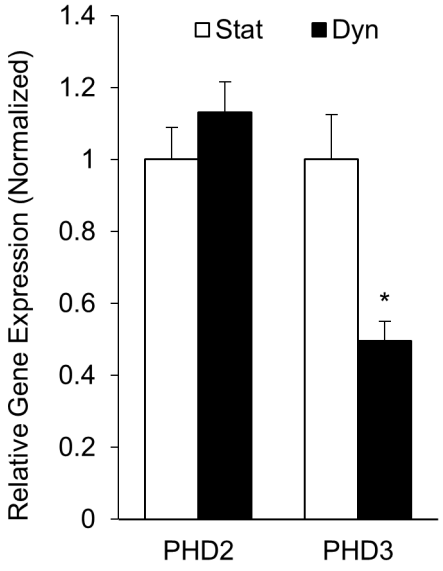

Figure S6: Hypoxia markers in NRVM cardiobundles.
Expression of prolyl hydroxylases PHD2 and PHD3 in NRVM cardiobundles cultured in static (Stat) or dynamic (Dyn) conditions for 14 days, normalized to Stat group. n = 7 samples per group from 2 cell isolations, each sample is 2 cardiobundles pooled together. * $p < 0.05$ compared to static.

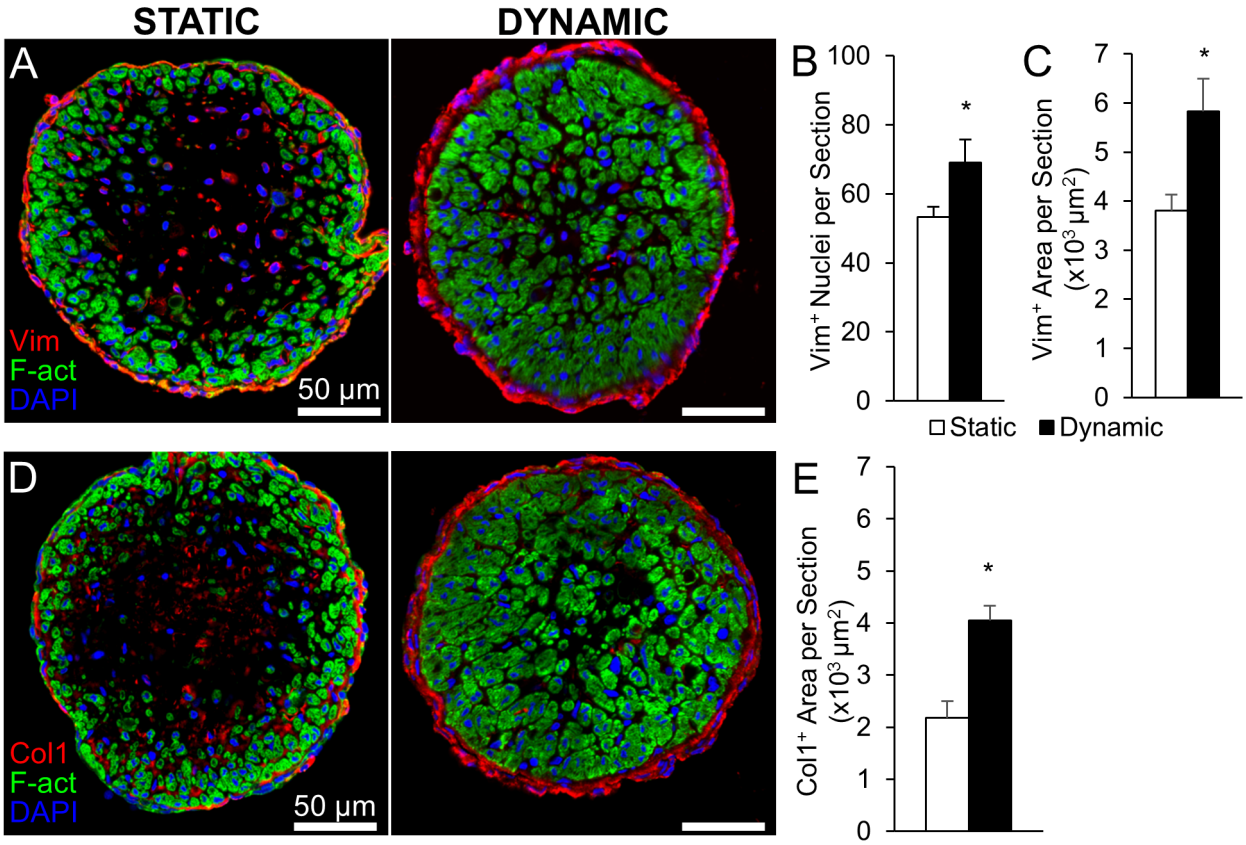

Figure S7: Cardiac fibroblasts and ECM in transverse cross-sections of NRVM cardiobundles. **(A)** Representative cross-sections of 2-week NRVM cardiobundles cultured under static or dynamic conditions, stained for vimentin (Vim, red), filamentous actin (F-act, green), and nuclei (DAPI, blue). **(B)** Number of vimentin-positive (Vim^+) nuclei counted in transverse cross-sections described in panel (A). **(C)** Quantification of the Vim^+ area in cross-sections described in panel (A). **(D)** Representative cross sections of 2-week cardiobundles stained for collagen I (Col1, red), filamentous actin (F-act, green), and nuclei (DAPI, blue). **(E)** Quantification of the $Col1^+$ area in cross sections described in panel (D). n = 9-10 cardiobundles per group from 3 cell isolations for (B – C); n = 5 cardiobundles per group from 2 cell isolations for (E). * $p < 0.05$ vs. static.

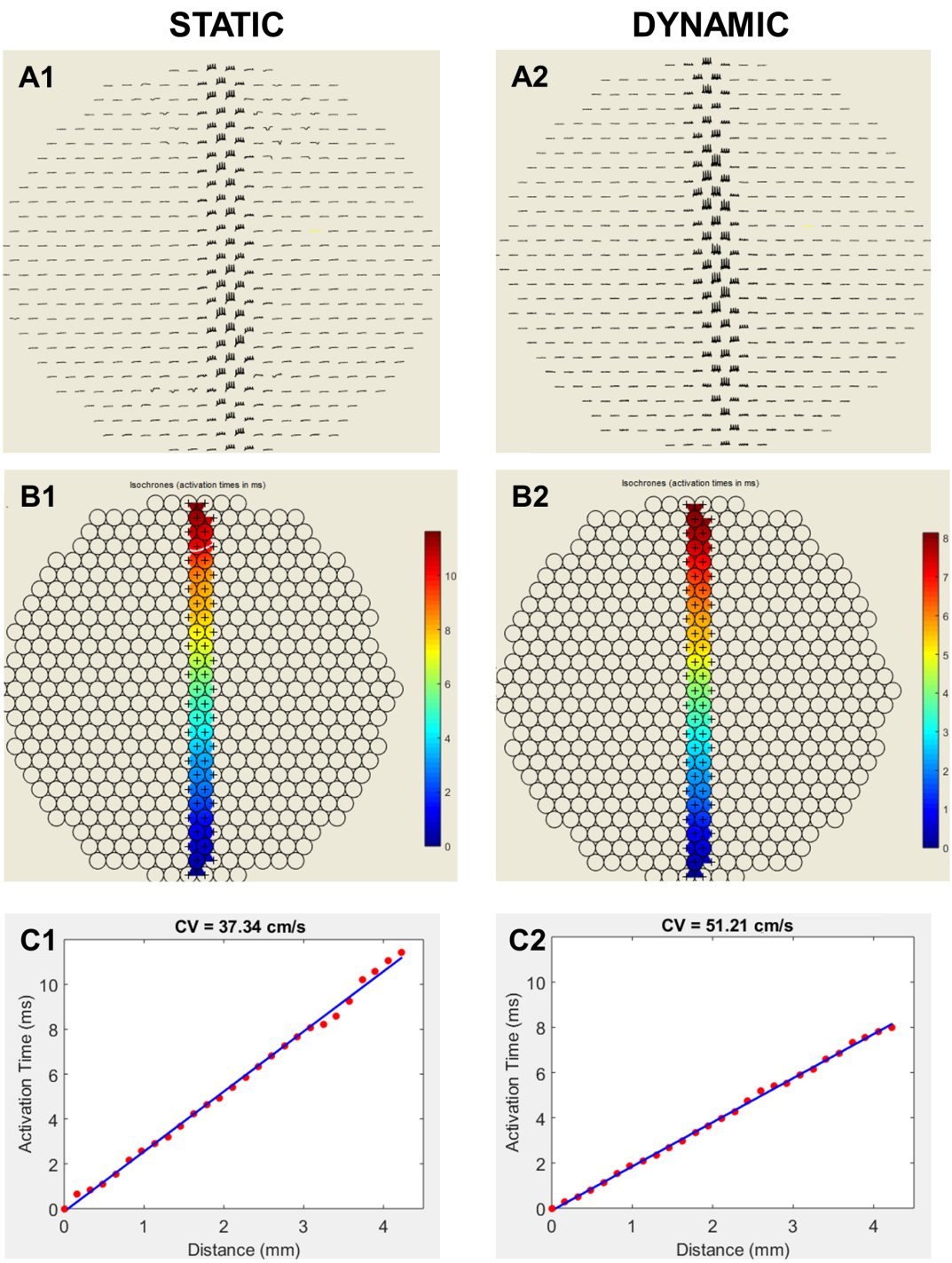

Figure S8: Measurement of conduction velocity (CV) in cardiobundles.
(A) Representative fluorescence vs. time recordings for 512 channels of the photo diode array, in response to applying 2 Hz suprathreshold point stimulus to static (A1) or dynamic (A2) 2-week NRVM cardiobundles stained with di-4 ANEPPS. **(B)** Activation times extracted from the recordings in the cardiobundle region were used to generate activation map plots. Channel (circle) diameter = 187.5 µm. **(C)** Plot of activation time vs. distance for each row of channels (red dots). Linear fit is shown as a blue line. CV was calculated as the inverse of the slope of the linear fit.

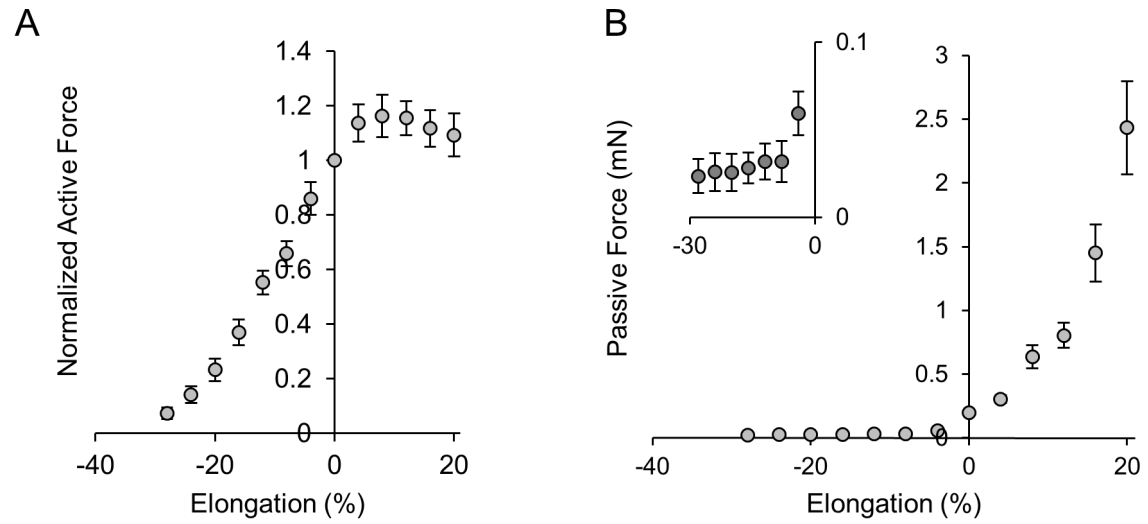

Figure S9: Complete active and passive force-length relationships in dynamically cultured NRVM cardiobundles.
(A) Normalized active force (relative to active force at baseline culture length) vs. cardiobundle elongation (assigned 0% at baseline culture length) in 2-week dynamically cultured NRVM cardiobundles. **(B)** Passive force vs. cardiobundle elongation. Inset shows close-up of passive force values for negative elongations (i.e., less than baseline culture length). These curves demonstrate physiological force responses to tissue elongation characterized by significant increase followed by decline of contractile force (A) and exponential increase of passive force (B).

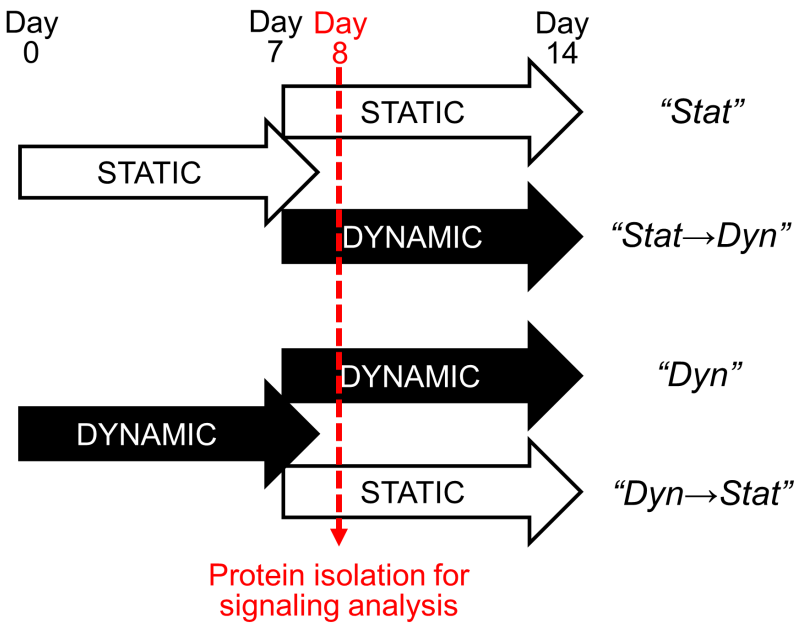

Figure S10: Experimental design for switching between static and dynamic culture midway through 2-week experiment.
Cardiobundles cultured statically or dynamically for the first 7 days were either kept in the same culture condition or switched to the opposite culture condition for the next 7 days. For experiments involving analysis of intracellular kinase signaling in NRVM cardiobundles, protein isolation was performed 24 hours after switch of culture condition.

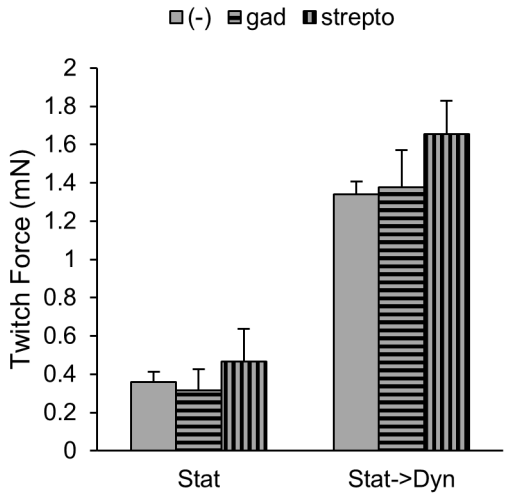

Figure S11: Effects of inhibiting stretch-activated channels in NRVM cardiobundles.
Max twitch force of cardiobundles cultured statically for 14 days (Stat) or cultured statically for 7 days then dynamic for 7 days (Stat→Dyn). Indicated drug was applied from culture day 7 to day 14: 20 μM gadolinium (gad) or 50 μM streptomycin (strepto) (n = 8-10 cardiobundles per group from 2 cell isolations).

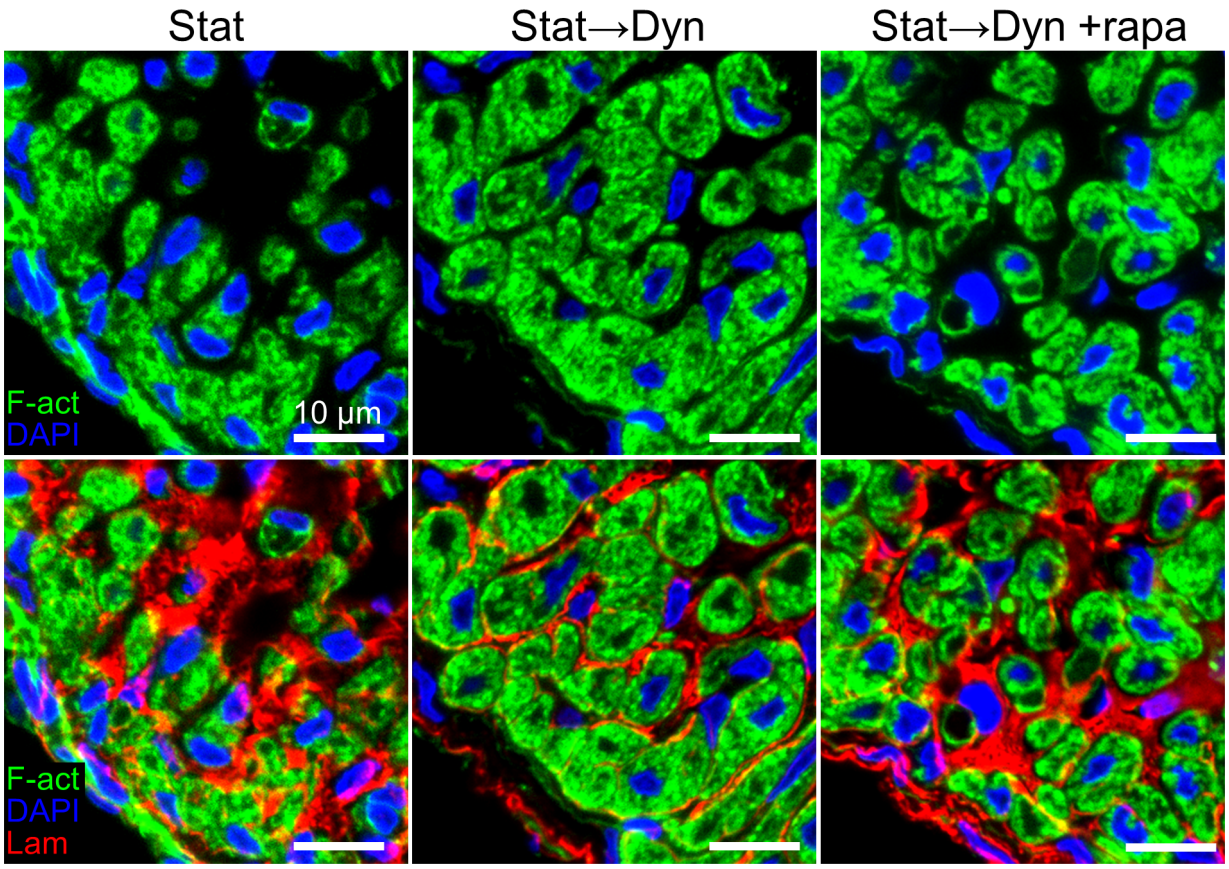

Figure S12: Attenuation of dynamic culture-induced CM hypertrophy by mTORC1 inhibition. Representative transverse cross-sections of 2-week NRVM cardiobundles cultured (left) statically (Stat), (middle) statically for 7 days followed by dynamically for additional 7 days (Stat→Dyn), and (right) statically for 7 days followed by dynamically for additional 7 days with 500 nM rapamycin (Stat→Dyn + rapa). Cross-sections were stained for filamentous actin (F-act, green), nuclei (DAPI, blue), and laminin (Lam, red, shown in second row). Images show the outer boundary, with area outside of cardiobundles visible in bottom-left corner. Note that rapamycin attenuated CM hypetrophy induced by dynamic culture, which was also visible from the relative increase in laminin-labeled extracellular area.

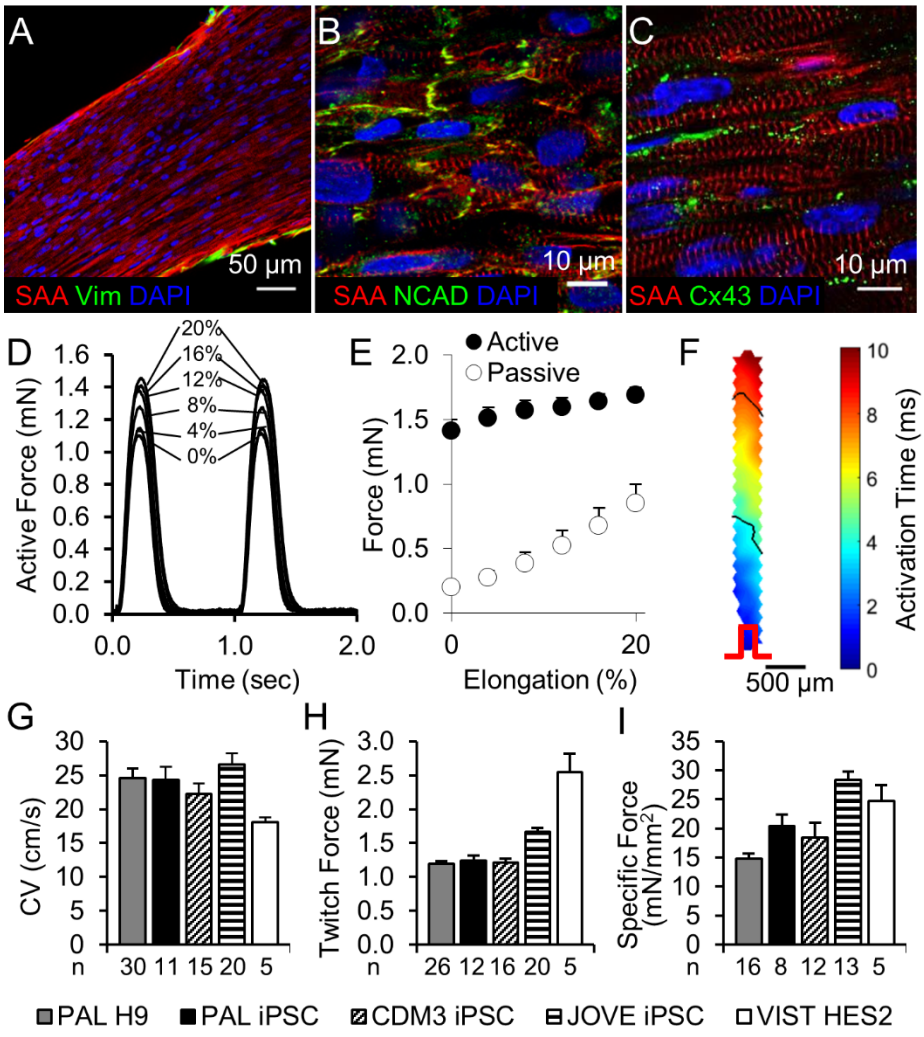

Figure S13: Structure and function of dynamically cultured human cardiobundles from various hPSC lines.

Representative images of human cardiobundles cultured for 3 weeks in dynamic conditions, stained for sarcomeric α-actinin (SAA, red), nuclei (blue), and **(A)** vimentin (Vim, green), **(B)** N-cadherin (NCAD, green), and **(C)** connexin 43 (Cx43, green). **(D)** Representative force traces for human microbundles at progressively longer stretch (shown in % of culture length). **(E)** Representative force-length curves. **(F)** Isochrone map displaying AP propagation with a high conduction velocity (CV = 42.1 cm/s) achieved in cardiobundles. **(G-I)** Summary of **(G)** CV, **(H)** max twitch force, and **(I)** max specific force for human cardiobundles made using CMs derived from various PSC lines and differentiation protocols (PAL = Palecek protocol, JOVE = S. Wu protocol, CDM3 = J. Wu protocol, VIST = Vistagen-provided cells). Numbers of analyzed cardiobundles (n) were shown below the individual bars.

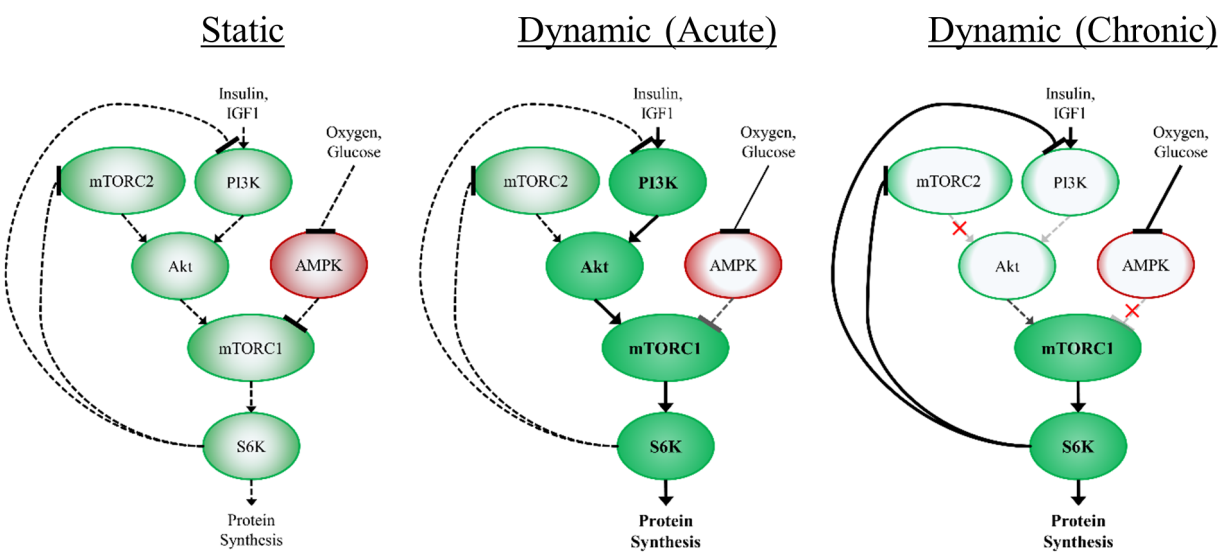

Figure S14: Proposed mechanism of cardiomyocyte growth in response to dynamic culture of engineered cardiobundles.
Proposed simplified mTOR signaling network based on the results shown in the main Fig. 6. Left, static culture showing basal activity of each kinase. Middle, after 24 hours of dynamic culture, activation of Akt, likely by insulin-IGF1/PI3K pathway; promotes mTORC1/S6K activity. Right, in chronic dynamic culture, negative feedback of S6K on mTORC2 and on PI3K-mediated insulin signaling suppresses Akt, but mTORC1 activation is maintained by suppression of AMPK. Both Akt and AMPK control mTORC1 through the intermediates TSC1/2 and Rheb GTPase (not shown); AMPK also directly inhibits mTORC1.